The inverse cascade of magnetic helicity in magnetohydrodynamic turbulence

Wolf-Christian Müller,[*] Shiva Kumar Malapaka,[†] and Angela Busse[‡]

Max-Planck-Institut für Plasmaphysik, 85748 Garching, Germany

The nonlinear dynamics of magnetic helicity, H^M, which is responsible for large-scale magnetic structure formation in electrically conducting turbulent media is investigated in forced and decaying three-dimensional magnetohydrodynamic turbulence. This is done with the help of high resolution direct numerical simulations and statistical closure theory. The numerically observed spectral scaling of H^M is at variance with earlier work using a statistical closure model [Pouquet et al., J. Fluid Mech. **77** 321 (1976)]. By revisiting this theory a universal dynamical balance relation is found that includes effects of kinetic helicity, as well as kinetic and magnetic energy on the inverse cascade of H^M and explains the above-mentioned discrepancy. Considering the result in the context of mean-field dynamo theory suggests a nonlinear modification of the α-dynamo effect important in the context of magnetic field excitation in turbulent plasmas.

The emergence of large-scale magnetic structures in turbulent plasmas is dynamically important in many astrophysical settings, e.g. with regard to the interstellar medium or the magnetic field generation in planets and stars by the turbulent dynamo effect, e.g. [1–3]. The structure formation can be studied via the magnetic helicity $H^{\mathrm{M}} = \frac{1}{2V} \int_V dV \mathbf{a} \cdot \mathbf{b}$ where $\mathbf{b}$ is the magnetic field and $\mathbf{a}$ denotes the magnetic vector potential. This topological characteristic of magnetic fields yields a measure of the linkage and the twist of the field lines, [4, 5]. In the magnetohydrodynamic (MHD) single-fluid approximation [6] which neglects microscopic scales and the associated kinetic dynamics H^{M} is ideally conserved in a three-dimensional volume with periodic or closed boundary conditions [7]. It is thus prone to a nonlinear and conservative inverse spectral cascade process in the inertial range of MHD plasma turbulence. If driven at small scales, ℓ, the cascade results in spectral transfer of magnetic helicity towards small spatial wavenumbers $k \sim \ell^{-1}$ [8], i.e. to the formation of large-scale magnetic structures. This process is thus of fundamental importance with regard to, e.g., the dynamics of magnetic fields in the above-mentioned turbulent astrophysical settings. In spite of its importance little is known about the nonlinear dynamics which underlies the inverse cascade. It is the purpose of this work to shed some light on the rather mysterious nonlinear phenomenon creating large-scale order out of quasi-random turbulent magnetic fluctuations. Please note that the constraining effect of magnetic helicity conservation on certain α-dynamo configurations is, although important, beyond the scope of this work, cf., for example, [9]. The existence of such an inverse cascade was first demonstrated in numerical simulations based on the eddy damped quasi normal Markovian (EDQNM) closure model of three-dimensional MHD turbulence [10] which is to the best of our knowledge the only work dealing theoretically with the spectral self-similarity of magnetic helicity. The associated self-similar spectral signature in the turbulent inertial range, $\sim k^{-2}$, is in agreement with dimensional analysis based on a constant nonlinear spectral flux. Several studies applying direct numerical simulations (DNS) find inverse transfer of magnetic helicity, see e.g. [11–13], without reporting self-similar scaling behaviour, a notable exception being [13].

In this Rapid Communication the inverse cascade of magnetic helicity in homogeneous MHD turbulence is studied by three-dimensional high-resolution direct numerical simulations. In the main setup kinetic and magnetic energy and magnetic helicity are injected at small scales of the initially excited spectral range of turbulent fluctuations. It is shown that macroscopic quantities, in particular kinetic helicity and the ratio of kinetic and magnetic energy, have an important influence on the H^{M}-cascade that is captured by a universal relation based on dimensional analysis of the MHD-EDQNM closure model. This insight suggests a new link between magnetic helicity and mean-field dynamo theory in particular with regard to the saturation behaviour of the dynamo mechanism.

The dimensionless MHD equations are written as

$$\partial_t \boldsymbol{\omega} = \nabla \times (\mathbf{v} \times \boldsymbol{\omega} + \mathbf{j} \times \mathbf{b}) + (\mu_n(-1)^{n-1}\Delta^n + \lambda\Delta^{-2})\boldsymbol{\omega} + \mathbf{F_v}, \tag{1}$$

$$\partial_t \mathbf{b} = \nabla \times (\mathbf{v} \times \mathbf{b}) + (\eta_n(-1)^{n-1}\Delta^n + \lambda\Delta^{-2})\mathbf{b} + \mathbf{F_b}, \tag{2}$$

$$\nabla \cdot \mathbf{v} = \nabla \cdot \mathbf{b} = \mathbf{0}, \tag{3}$$

where $\mathbf{v}$ is the velocity, $\boldsymbol{\omega} = \nabla \times \mathbf{v}$ the vorticity, $\mathbf{b}$ the magnetic field, and $\mathbf{j} = \nabla \times \mathbf{b}$ the electric current density. Equations (1)–(3) are solved by a standard pseudospectral method using a leapfrog scheme for time integration. Anti-aliasing is achieved by spherical mode truncation. The simulation domain is a triply 2π-periodic cube discretized by 1024^3 collocation points. Hyperviscous small-scale dissipation operators of order $n = 8$ are used to improve scale separation parametrized by the hyperdiffusion coefficients μ_n and η_n with the hyperviscosity $\mu_8 = 9 \cdot 10^{-41}$ and $\mu_8/\eta_8 = 1$. Boundary effects at
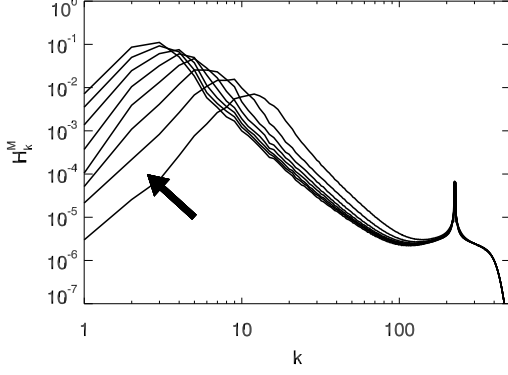
FIG. 1: Inverse cascade of magnetic helicity, H_k^{M}, in 3D-MHD turbulence for $t \in [1, 6.66]$. Curves are given for points in time spread equidistantly over the interval. Magnetic fluctuations with maximal magnetic helicity and non-helical velocity fluctuations are supplied through the forcing with $k_0 = 206$.
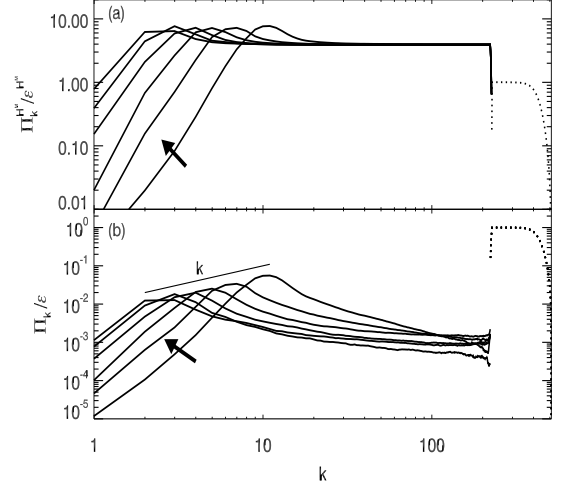

FIG. 2: Moduli of fluxes of magnetic helicity (a) and total energy (b) (inverse: solid curves, direct: dotted curves) normalized by corresponding dissipation rates. Flux spectra are shown for $t \in [1.66, 6.66]$ for the forced simulation and are spread equidistantly over this period.

smallest spatial wavenumbers k are alleviated by a large-scale energy sink $\lambda\Delta^{-2}$ for both fields with the constant λ set to 0.5. The forcing terms $\mathbf{F_v}$ and $\mathbf{F_b}$ are random, delta-correlated processes of equal amplitude that act over a band of wave numbers $k \in [k_0 - 3, k_0 + 3]$ with $k_0 = 206$. They inject velocity- and magnetic-field fluctuations with well defined magnetic and kinetic helicity, kinetic helicity being defined as $H^K = \frac{1}{2V}\int_V dV \mathbf{v}\cdot\boldsymbol{\omega}$. Such driving, chosen here for simplicity and numerical efficiency, could in principle be realized by a random small-scale distribution of electric currents and forces. The initial velocity and magnetic fields are smooth with equal energies, random phases and fluctuations that have a Gaussian energy distribution, peaked at k_0. In the course of the simulation the total energy quickly attains a quasi-stationary state, fluctuating around unity with $E^M/E^K \approx 9$. Cross-helicity, $H^C = \frac{1}{2V}\int_V dV \mathbf{v}\cdot\mathbf{b}$, is negligible. The simulation is carried up to t=6.66 large-eddy turnover times. The application of hyperviscous dissipation operators while necessary to observe well-developed scaling ranges precludes the unambiguous definition of a Reynolds number.

The temporal evolution of the magnetic helicity spectrum over the simulation period shown in Fig. 1 indicates inverse spectral transfer. This is also reflected by the nonlinear spectral flux of magnetic helicity, $\Pi_k^{H^M} = 2\int_0^k dk' k'^2 \int d\Omega (\mathbf{b}_{\mathbf{k}'}^* \cdot [\mathbf{v}\times\mathbf{b}]_{\mathbf{k}'} + \text{c.c.})$ with '$[\bullet]_\mathbf{k}$' denoting Fourier transformation and '$*$' standing for complex conjugate (c.c.). The flux spectrum shown in Fig. 2(a), is constant over finite wavenumber intervals on both sides of the forcing band signalling equilibrium between turbulence driving and dissipation. While on the right-hand-side direct spectral transfer is observed as a result of the small-scale energy sink, on the left-hand-side of the forcing band an inverse cascade de-

velops which is driven by the constant magnetic helicity input around k_0. The spectral flux of total energy, $E = E^K + E^M = \int d^3k(|v_\mathbf{k}|^2 + |b_\mathbf{k}|^2)/2$, is given by $\Pi_k = \int_0^k dk' k'^2 \int d\Omega(i\mathbf{k}' \times [\mathbf{v}\times\boldsymbol{\omega} + \mathbf{j}\times\mathbf{b}]_{\mathbf{k}'} \cdot \mathbf{v}_{\mathbf{k}'}^* + i\mathbf{k}' \times [\mathbf{v}\times\mathbf{b}]_{\mathbf{k}'} \cdot \mathbf{b}_{\mathbf{k}'}^* + \text{c.c.})$ and is shown in Fig. 2(b). It lacks spectral constancy in the inverse cascade region and it is principally carried by magnetic energy transfer. This suggests that the inverse energy flux is a consequence of the inverse cascade of H^M. The linear scaling of the Π_k-envelope which follows from the dimensional estimate $E_k \sim kH_k^{\mathrm{M}}$ in combination with the approximate constant value of the envelope of $\Pi_k^{H^M}$ also supports this interpretation.

The compensated magnetic helicity spectrum at the end of the simulation period is displayed in Fig. 3(a). It exhibits two approximate scaling ranges: on the direct transfer side for $250 \lesssim k \lesssim 400$ and in the inverse transfer region, $7 \lesssim k \lesssim 30$. The corresponding asymptotic scaling laws are $H_k^{\mathrm{M}} \sim k^{-3.3}$ (inverse, cf. [13]) and $H_k^{\mathrm{M}} \sim k^{-1.5}$ (direct). The latter value has to be taken with care due to the very short spectral range and the high-order hyperviscosity acting at largest wavenumbers. The inverse cascade scaling is at variance with the k^{-2}-behaviour reported in [10].

Since H^{M} is the helicity of the magnetic vector potential, $\mathbf{a}$, its inverse cascade pulls quantities derived from this potential, e.g. magnetic energy and to a lesser extent also electric current density, $\mathbf{j}_k \sim k^2\mathbf{a}_k$, towards large scales. Magnetic and velocity field are intrinsically coupled in MHD turbulence by Alfvénic fluctuations [14] and thus similar behaviour is observed for the spectral kinetic energy and kinetic helicity, H_k^{K}, as well. The respective
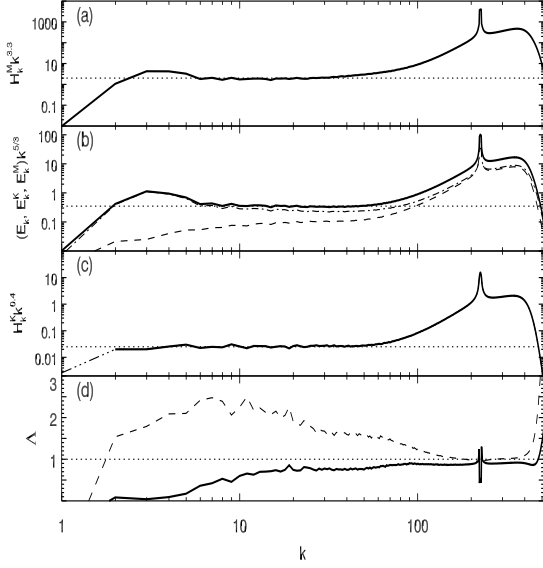
FIG. 3: Compensated spectra of (a) magnetic helicity , (b) total (solid line), kinetic (dashed line), magnetic (dashed-dotted line) energy, (c) kinetic helicity. (d) $\Lambda = (E_k^K/E_k^M)^\gamma H_k^J/H_k^K$ for $\gamma = 1$ (dashed line) and $\gamma = 2$ at t=6.66 in the driven simulation.

spectra are thus expected to inherit the self-similarity from H_k^M as is indeed observed, see, e.g., Fig. 3(c). It seems to be reasonable to regard the merging of current-carrying structures where the currents have significant positively aligned components and thus experience mutual attraction as the physical mechanism of the inverse cascade of magnetic helicity, cf. [15]. This is also in line with recent statements in the literature about non-locality of the magnetic helicity flux [12, 16].Terming the inverse transfer of H_k^M a "cascade" is thus merely following convention and not a physical description of the actual process of a spectrally non-local merging of current-carrying strucures. Note that in this simulation no kinetic helicity is injected by the turbulence driving. In the case of simultaneous injection of kinetic helicity the spectral diagnostics discussed in this work show no significant difference to the presented simulations. In general the details of the small-scale forcing, like randomness of amplitude and/or complex phases, were verified to have no measureable impact on the self-similar behavior reported below. The only significant parameter in this respect is the separation of the smallest admissible wavenumber, $k = 1$, and the forcing-wavenumber of about two decades. The scale-separation determines the extent of the observable self-similar inverse-cascade dynamics. It is thus even more important than the classical Reynolds number which is not well defined due to the necessary high-order hyperviscous small-scale diffusion.

The energy spectra in Fig. 3(b) exhibit approximate scaling known from decaying turbulence, cf., e.g., [14, 17],

i.e. $E_k \sim k^{-5/3}$ and $E_k^R = |E_k^M - E_k^K| \sim k^{-7/3}$ (not shown) with an excess of magnetic energy. The observations are in agreement with the interpretation of the finite levels of E_k^K and of H_k^K as a result of the local and temporary stirring induced by changes of magnetic-field topology. This is to be expected in the course of the inverse cascade of magnetic helicity. As will be shown in the following, the lacking equipartition of E_k^K and E_k^M and the presence of kinetic helicity are the reasons of disagreement with the above-mentioned EDQNM simulations of [10]. There, the relaxation time of nonlinear interaction, θ_{kpq}, which represents a free parameter of the EDQNM approach and determines the nonlinear process governing turbulent dynamics, is chosen to be the Alfvén time, $(kB_0)^{-1}$. Consequently, the resulting dominance of Alfvénic interactions drives the system in the inertial range into nearly perfect equipartition of kinetic and magnetic energies.

The observed spectral scaling of magnetic helicity can be better understood with the help of the integro-differential EDQNM equation for the evolution of H_k^M. A formally similar approach has been successful with regard to the residual energy spectrum $E_k^R = |E_k^M - E_k^K|$ [14]. The equation for the evolution of H_k^M in the EDQNM model [10] reads

$$(\partial_t + \eta_1 k^2)H_k^M = \int_\triangle dp dq \theta_{kpq}(T_k^{\mathrm{adv}} + T_k^{\mathrm{khl}} + T_k^{\mathrm{lor}}) \quad (4)$$

with

$$
\begin{aligned}
T_k^{\mathrm{adv}} &= h_{kpq}\frac{k}{pq}(k^2 E_q^K H_p^M - p^2 E_q^K H_k^M)\,, \\
T_k^{\mathrm{khl}} &= h_{kpq}\frac{k}{pq}\left(\frac{k^2}{p^2}E_q^M H_p^K - \frac{k^2}{p^2}E_k^M H_q^K\right), \\
T_k^{\mathrm{lor}} &= e_{kpq}\frac{p^2}{k}E_k^M H_q^M - j_{kpq}\frac{kp}{q}E_q^M H_k^M\,.
\end{aligned}
$$

The geometric coefficients h_{kpq}, e_{kpq}, and j_{kpq} follow from the solenoidality constraints (3) and are given in [10]. The '$\triangle$' restricts integration to wave vectors $\mathbf{k}$, $\mathbf{p}$, $\mathbf{q}$ which form a triangle, i.e. to a domain in the p-q plane which is defined by $q = |\mathbf{p} + \mathbf{k}|$. The time θ_{kpq} is characteristic of the eddy damping of the nonlinear energy flux involving wave numbers k, p, and q. It is defined phenomenologically but its particular form does not play a role in the following arguments.

The three nonlinear contributions on the right-hand-side of Eq. (4) can be associated with the advective (T_k^{adv}) and explicitly twisting (T_k^{khl}) effects of turbulent fluctuations, as well as self-interaction (T_k^{Lor}) of the magnetic field through the Lorentz force. Assuming that the most important nonlinearities involve the turbulent velocity and that the spectral scaling range of H_k^M is stationary, a dynamical equilibrium of turbulent advection and the H^M-increasing effect of helical fluctuations is assumed, i.e. $T_k^{\mathrm{adv}} \sim T_k^{\mathrm{khl}}$. Dimensional approximation of

the respective flux terms, $kE_k^K H_k^M \sim k^{-1}E_k^M H_k^K$, yields

$$H_k^K \sim \left(\frac{E_k^K}{E_k^M}\right)^\gamma k^2 H_k^M, \quad \gamma = 1. \tag{5}$$

This is a statement about the spectral dynamics of kinetic and magnetic helicities (or kinetic and current helicities, $H^J = \frac{1}{2V}\int_V (\nabla \times \mathbf{b}) \cdot \mathbf{b}$, since $H_k^J \sim k^2 H_k^M$) in the case of $E_k^K/E_k^M \neq 1$. The agreement of Rel. (5) with the numerical experiment is significantly improved, see Fig. 3(d), when increasing γ by one. This yields the main result

$$H_k^K \sim \left(\frac{E_k^K}{E_k^M}\right)^2 H_k^J. \tag{6}$$

Rel. (6) is fulfilled, i.e. constant and close to unity, for almost all wavenumbers $k > 12$ excluding the drive and deep dissipation scales. It does however not cover the full spectral scaling range of H_k^M due to its susceptibility to the asymmetry of energies and helicities introduced by the large-scale energy sink. The higher-order modification of Rel. (5) can not be motivated within the framework of quasi-normal EDQNM theory using the chosen approach of nonlinear equilibrium. The underlying cause is presumably the non-locality of the inverse cascade process which is not captured by the dimensional simplification of the EDQNM equations.

For verification purposes a test simulation of decaying turbulence with the same numerical resolution of 1024^3 and an initially finite level of magnetic helicity, i.e. 50% of the energetically possible maximum $H_{\max}^M \sim E^M/k_0$, is conducted. The initial Gaussian random-phase energy spectrum with $E_k^K = E_k^M$ for all k is peaked around $k_0 = 70$ to allow some development of inverse transfer. The distribution of H_k^M is homogeneous over the initial spectrum. The hyperdiffusive coefficients are chosen as $\mu_8 = \eta_8 = 3 \cdot 10^{-41}$ with forcing switched off. Fig. 4 displays the most important results of this decaying test simulation after about 9.2 large-eddy turnover times. The magnetic helicity, Fig. 4(a), exhibits approximate self-similar spectral scaling $\sim k^{-3.6}$ with most of the excited scales in the range $15 \lesssim k \lesssim 60$ having developed during the decay. Kinetic helicity, see Fig. 4(b), reflects this as it is not injected into the system but generated via the Lorentz force during the inverse transfer of H_k^M. It shows two distinct asymptotic power-laws: $\sim k^{-0.5}$ for $60 \lesssim k \lesssim 120$ and $\sim k^{0.4}$ for $11 \lesssim k \lesssim 45$ in the range covered by the inverse transfer of H_k^M during turbulence decay. The signatures of kinetic, magnetic and total energies are similar to the observation made in the driven case. The spectral flux of magnetic helicity, Fig. 4(c), exhibits a split near k_0 as for $k > k_0$ small-scale dissipation determines the helicity transfer direction while for $k < k_0$ an inverse transfer with k-dependent $\Pi_k^{H^M}$ is observed. This is reflected by Rel. (6), cf. Fig. 4(d),
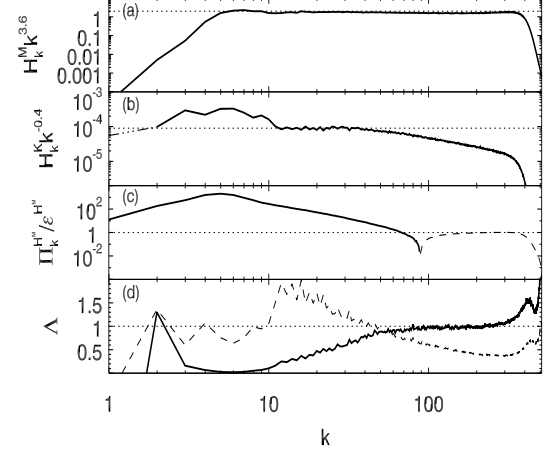

FIG. 4: Compensated spectra of (a) magnetic helicity , (b) kinetic helicity. (c) Spectral magnetic helicity flux normalized by corresponding dissipation rate (Inverse: solid curve, direct: dashed curve). (d) $\Lambda = (E_k^K/E_k^M)^\gamma H_k^J/H_k^K$ for $\gamma = 1$ and scaled by a factor $1/3$ (dashed) and for $\gamma = 2$. All spectra shown have been taken at $t = 9.2$ in the decaying simulation.

which is only fulfilled in the region of approximately constant $\Pi_k^{H^M}$ and is apparently independent of the transfer direction.

Comparison of the presented findings with mean-field dynamo theory, cf., for example, [3] and references therein, in particular the α-coefficient including the current helicity, $\alpha \sim H^J - H^K$, is interesting. Rel. (6) is consistent with vanishing α since the cascade process does not generate magnetic flux and, thus, does not act as a dynamo itself. It furthermore suggests a modified $\alpha \sim (E^K/E^M)^2 H^J - H^K$ which includes the squared ratio of kinetic and magnetic energy $\sim (E^M)^{-2}$ as a turbulent dynamo-quenching mechanism of the current helicity contribution to α. This form of α-quenching has recently been observed in a numerical test-field model [18].

In summary a new and probably universal relation connecting the spectral behaviour of magnetic and kinetic helicities and energies in homogeneous MHD turbulence is found motivated by statistical EDQNM closure results. DNS of MHD turbulence that is decaying or driven at small scales confirm the validity of the findings for spectral intervals of constant flux of magnetic helicity. The result has interesting connections to the α coefficient known from mean-field dynamo theory: it suggests an inherent and strong quenching of the dynamo, in particular of the current helicity effect, if the energy of turbulent magnetic fluctuations grows compared to the kinetic contribution of velocity.

* Electronic address: wolf.mueller@ipp.mpg.de

† Electronic address: shiva.kumar.malapaka@ipp.mpg.de; Now at:University of Leeds, Faculty of Mathematics and Physical Sciences, United Kingdom

‡ Electronic address: a.busse@soton.ac.uk; Now at:University of Southampton, Faculty of Engineering and the Environment, United Kingdom

[1] A. M. Soward, C. A. Jones, D. W. Hughes, and N. O. Weiss, eds., *Fluid Dynamics and Dynamos in Astrophysics and Geophysics*, Durham Symposium on Astrophysical Fluid Mechanics 2002 (CRC Press, Boca Raton, Florida, 2005).

[2] R. M. Kulsrud and E. G. Zweibel, Reports on Progress in Physics **71**, 046901 (2008).

[3] A. Brandenburg and K. Subramanian, Physics Reports **417**, 1 (2005).

[4] H. K. Moffatt, Journal of Fluid Mechanics **35**, 117 (1969).

[5] M. A. Berger and G. B. Field, Journal of Fluid Mechanics **147**, 133 (1984).

[6] D. Biskamp, *Nonlinear Magnetohydrodynamics* (Cambridge University Press, Cambridge, 1993).

[7] L. Woltjer, Proceedings of the National Academy of Sciences **44**, 833 (1958).

[8] U. Frisch, A. Pouquet, J. Léorat, and A. Mazure, Journal of Fluid Mechanics **68**, 769 (1975).

[9] A. Brandenburg, Space Science Reviews **144**, 87 (2009).

[10] A. Pouquet, U. Frisch, and J. Léorat, Journal of Fluid Mechanics **77**, 321 (1976).

[11] A. Brandenburg, The Astrophysical Journal **550**, 824 (2001).

[12] A. Alexakis, P. Mininni, and A. Pouquet, The Astrophysical Journal **640**, 335 (2006).

[13] P. Mininni and A. Pouquet, Physical Review E **80**, 025401 (2009).

[14] W.-C. Müller and R. Grappin, Physical Review Letters **95**, 114502 (2005).

[15] D. Biskamp und U. Bremer, Physical Review Letters **72**, 3819 (1993).

[16] H. Aluie and G. L. Eyink, Physical Review Letters **104**, 081101 (2010).

[17] W.-C. Müller and D. Biskamp, Physical Review Letters **84**, 475 (2000).

[18] M. Rheinhardt and A. Brandenburg, Astronomy & Astrophysics **520**, A28 (2010).